JOURNAL OF MATERIALS SCIENCE 22 (1987) 1013–1018

Structure, mechanical properties and fracture of aluminium alloy A-356 modified with Al–5Sr master alloy

NABIL FAT-HALLA
Mechanical Department, Faculty of Engineering, Al Azhar University, Cairo, Egypt

The cooling rate during solidification of the aluminium–silicon alloy A-356 was found to have a pronounced effect not only on the structure and mechanical properties, but also on the modification process using Al–5 mass % Sr master alloy. Cooling rates in the range of 0.2 to 5 K sec^{-1} were conducted using different types of moulds. Decreasing the cooling rate increases the degree of modification obtained, and a cooling rate of 0.2 K sec^{-1} showed the optimum modification in the present study. The mechanical properties were significantly improved by modification. Ductility of the modified alloy was eight times greater than that for the non-modified one. Moreover, the mechanical properties of the modified alloys, in the present study, were higher than those modified with sodium, and additionally the ductility of the present modified alloy was higher than that for alloys modified with strontium. A tendency towards ductile rupture was observed. The transgranular type of fracture was optically detected, and a dimple-pattern was observed on the fracture surface by scanning electron microscopy.

1. Introduction

The density of silicon is 2.3 kg dm^{-3} and that of aluminium 2.7 kg dm^{-3} so that silicon is one of the few elements which may be added to aluminium without loss of weight advantage. Additionally, the aluminium–silicon alloys are important foundry materials. Their importance arises because small (~ 0.01 mass %) concentrations of sodium produce a spectacular refinement of the scale and distribution of the phases, which is accompanied by a great improvement in the mechanical properties [1]. The refined structure is said to be "modified", and although the material is attractive because it has low specific gravity and good casting characteristics, it is the process of modification which makes the alloys economically significant.

In the Al–Si phase diagram given by Hansen [2], the composition of the eutectic point is 11.7 mass % Si, being the most consistent value found in the literature prior to 1958. Recent investigations [3, 4] have relocated the eutectic point at 12.5 $\pm$ 0.1 mass % Si. The maximum solubility of silicon in aluminium is 1.65 mass % at the eutectic temperature of 850 K. The aluminium-rich portion of the Al–Si phase diagram, based on the above data [5], is replotted in Fig. 1.

It is now well known [1, 3, 4, 6, 7] that the sodium content falls rapidly while the alloy is molten, so that to achieve a final concentration in the casting of 0.01%, as much as 0.1% of metallic sodium may be added to the melt. The loss of sodium is most rapid at higher temperatures, but at the same time, the addition is most effective if it is made at higher temperatures.

Owing to the practical difficulties mentioned above, and others, of modifying the aluminium–silicon alloys using sodium, the need for new modifiers arose. The present investigation is an attempt to modify the commercial alloy A356 using a recently produced Al–5 mass % Sr master alloy. Moreover, a study on the effect of such modification on the microstructure, mechanical properties and the fracture phenomena is to be carried out. Since the cooling rate during solidification is known to have a pronounced effect not only on the mechanical properties but also on the modification process itself [3, 4], the present research studied solidification under different cooling rates.

2. Experimental procedure

Experiments described in this work were conducted on A356 alloys with the following composition: silicon, 7%; iron, 0.01%; copper, 0.06%; magnesium, 0.30%; manganese, 0.05%; niobium, 0.14%; zinc, 0.05%; titanium, 0.14%; lead, 0.03%; tin, 0.04; strontium, nil and aluminium, balance.

The cooling rates during solidification were accurately measured using an alumel–chromel thermocouple connected to a digital counter and an x–t recorder. Table I delineates the different types of moulds used in the present study, and their

TABLE I Different types of moulds and their cooling rates*

Type of mould and conditions	Cooling rate (K sec^{-1})
Copper mould	5
Graphite mould (air cooled)	2
Graphite mould (preheated to 773 K)	0.6
Sand mould†	0.2

*All ingots were quenched into water after being solidified (i.e. quenched from the eutectic temperature 850 K).
†This mould was machined from firebrick.

0022–2461/87 $03.00 + .12

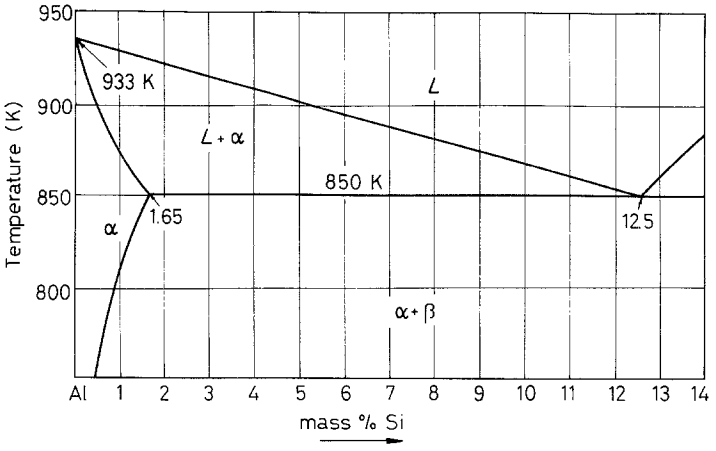

Figure 1 Aluminium-rich portion of the Al–Si phase diagram.

corresponding cooling rates (the mass of the ingot in all cases was approximately 70 g).

Fig. 2 is a schematic illustration of the mould used, together with its dimensions in mm (all types of moulds had the same shape and dimensions as shown in Fig. 2).

The strontium needed for optimum modification of the alloy A356 was found to be 0.02%. Accurately calculated mass of Al–5Sr master alloy was added to the molten metal at 970 K, manually stirred and then kept for about 0.3 ksec at the mentioned temperature and poured directly into the mould.

The tensile specimens were machined to a gauge diameter of 5 mm and gauge length of 10 mm. Tensile tests were conducted at a constant cross-head speed of 0.01 mm sec^{-1}. The fracture, due to tension, was studied by both optical and scanning microscopy.

3. Results and discussion

Fig. 3 shows the microstructure of the specimens cast in copper moulds. It consists of dendrites of primary α-phase (aluminium), with an average grain size of 25 μm, surrounded by the eutectic mixture of aluminium and silicon. As can be detected from Fig. 3, the volume fraction of the primary α-phase is about 72% of the whole alloy. This ratio is higher than that expected from the phase diagram shown in Fig. 1, under thermodynamic equilibrium conditions (~ 50%) This increase in α volume fraction indicates the shift of the eutectic point (cf. Fig. 1) to the right [3, 4], i.e. to a higher silicon content, owing to the fast cooling rate used in this group of specimens (5 K sec^{-1}). This result agrees with that published previously [4] in which the quenching of material of nominal eutectic composition not only influences the silicon dispersion, but also involves a shift in the composition of the fine structure to higher silicon contents as the incidence of aluminium dendrites increases.

The engineering stress–strain diagrams for the present group of specimens indicated an average yield strength of 125 MPa, tensile (and fracture) strength of 183 MPa, and elongation of 2.1%. A large scatter does exist in the tensile properties of this group, reflecting the brittleness of the specimens. The scatter for the yield and tensile strengths was ± 5% and that for the elongation was ± 20%. Trials to modify this group of specimens did not succeed. Information in the literature indicate that chill cast Al–Si eutectic could be modified by sodium and its mechanical properties were significantly improved [4]. On the other hand, recent researches [8, 9] on the modification of Al–Si–Mg alloy by a strontium element showed that the strontium level has little effect on structure at the highest cooling rate of 1.5 K sec^{-1}. At the slowest rate, 0.08 K sec^{-1}, there is a pronounced effect of strontium, since the solidification rate is near to the critical cooling rate for modification. Thus, strontium modification is more useful at lower cooling rates and should be a favoured method of modification in heavier section castings and in sand castings. To summarize, the

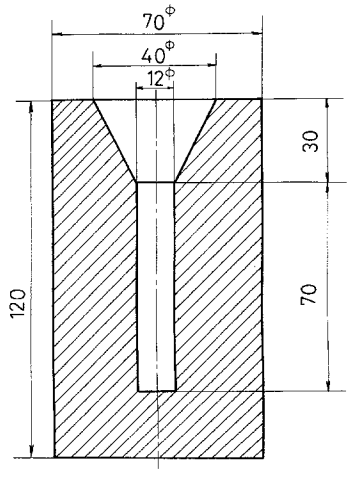

Figure 2 Schematic illustration of the mould together with its dimensions in mm.

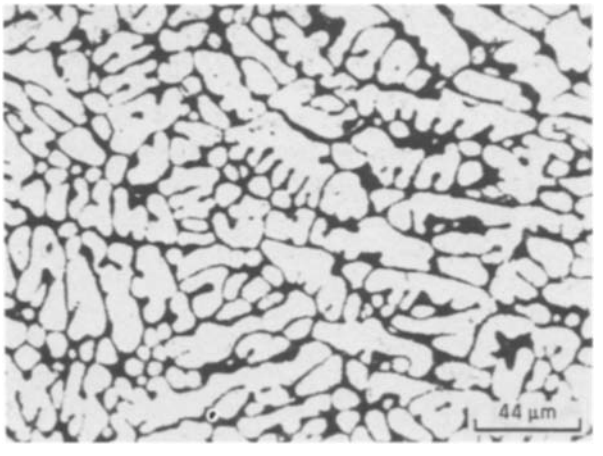

Figure 3 Microstructure of alloy A-356 cast in a copper mould.

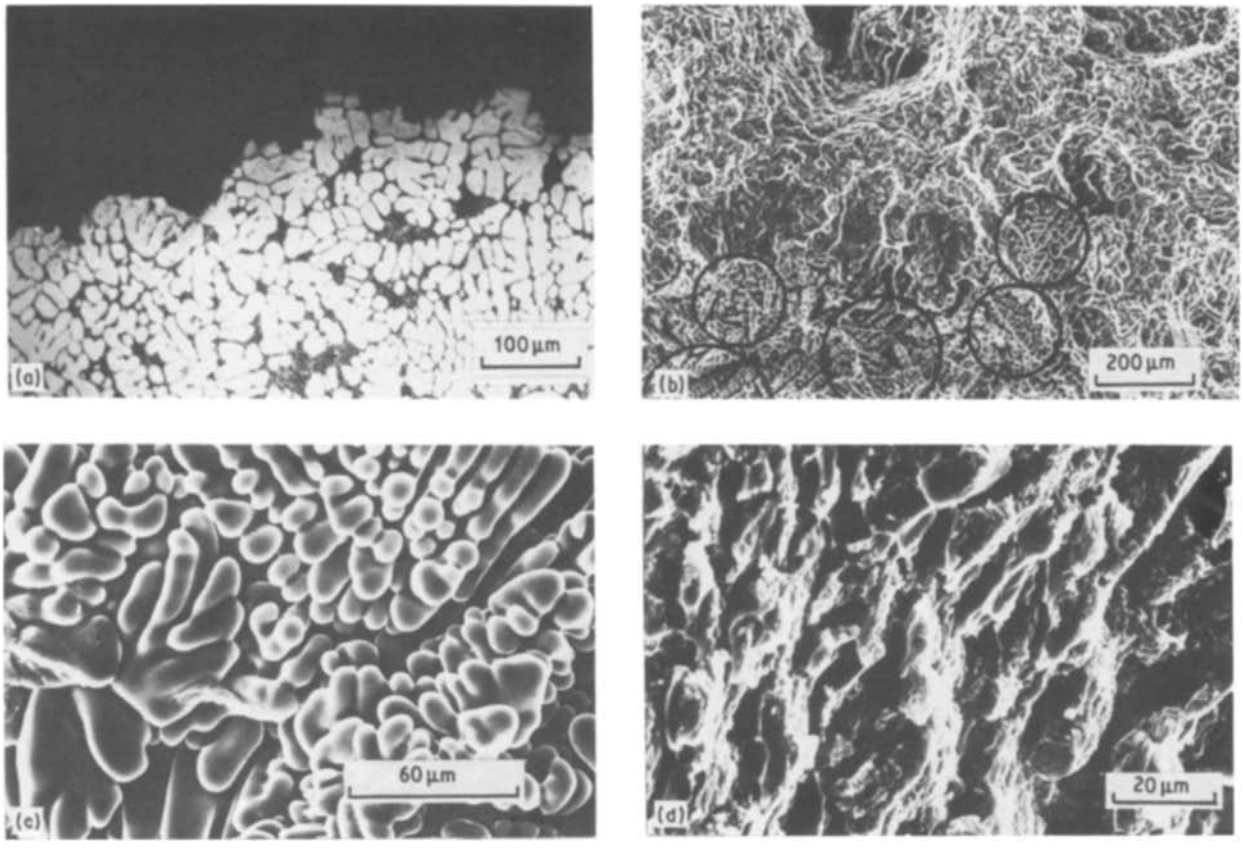

Figure 4 Fractography of alloy A-356 cast in a copper mould; (a) longitudinal section, (b) general features, (c) dendritic lobes, and (d) cellular structure.

cooling rate for the copper mould in the present research (5 K sec^{-1}) was higher than the critical cooling for modification by Al–5 mass % Sr master alloy.

Fig. 4a shows a longitudinal section of a sample specimen of this group, as observed by an optical microscope near the fracture surface. This photomicrograph shows an intergranular type of brittle fracture, and at the same time, it shows the fine eutectic structure resulting from the fast cooling rate (5 K sec^{-1}). Fig. 4b to d shows the features of the fracture surface as revealed by the scanning electron microscope. Fig. 4b delineates the general features observed at medium magnification, showing several regions of shrinkage porosity containing dendrite lobes, which existed as "free surfaces" within the cavities after the available liquid metal solidified (encircled areas). Fig. 4c shows an example of such regions at high magnification. These cavities could have been caused by entrapped air being carried into the mould by undue turbulence in pouring the casting, or due to the high cooling rate in this specific group (shrinkage porosity). The second feature shown in 4b is that shown at high magnification in Fig. 4d, which resembles a cellular structure. Additionally, this region does not contain any shrinkage porosity. The overall fracture generally lacked dimples and was brittle in nature.

Two main factors are believed to be responsible for the low ductility (2.1%) and brittleness (cf. Fig. 4) of the castings of this group in spite of their refined eutectic structure (fine eutectic structure is known to improve the ductility [4]). The first is due to the large "shrinkage porosity" observed on the fracture surface (cf. Fig. 4b). The latter is believed to refer to the morphology of the eutectic silicon (eutectic silicon in the present case, although fine, is sharp or angular).

The microstructure of sample specimens of alloys cast in a graphite mould are shown in Fig. 5a, b. In Fig. 5a, the alloys were air cooled, and the photomicrograph illustrates comparatively large primary α-phase dendrites (cf. Fig. 3) having an average grain size of about 50 μm, embedded in a fine eutectic matrix. This fine eutectic structure resulted from the relatively fast cooling rate of 2 K sec^{-1} (the ratio of this cooling rate to that of the highest value for the copper mould is 0.4). On the other hand, in Fig. 5b the alloys were cast in preheated graphite moulds (773 K); the microstructure here contains coarse acicular silicon. Attempts to modify both types cast in graphite moulds failed in the former case but succeeded in the latter. This success can clearly be seen from the photomicrograph in Fig. 6 in which "partial modification" could be achieved [7–10].

TABLE II The mechanical properties of alloy A-356 cast in a graphite mould

Number	Conditions	Yield strength, σ_y (MPa)	Ultimate tensile strength, σ_u (MPa)	Elongation (%)
1	Air cooled	150	240	6.2
2	Preheated (773 K)	114	155	1.75
3	Preheated + "modifier"	140	178	4.0

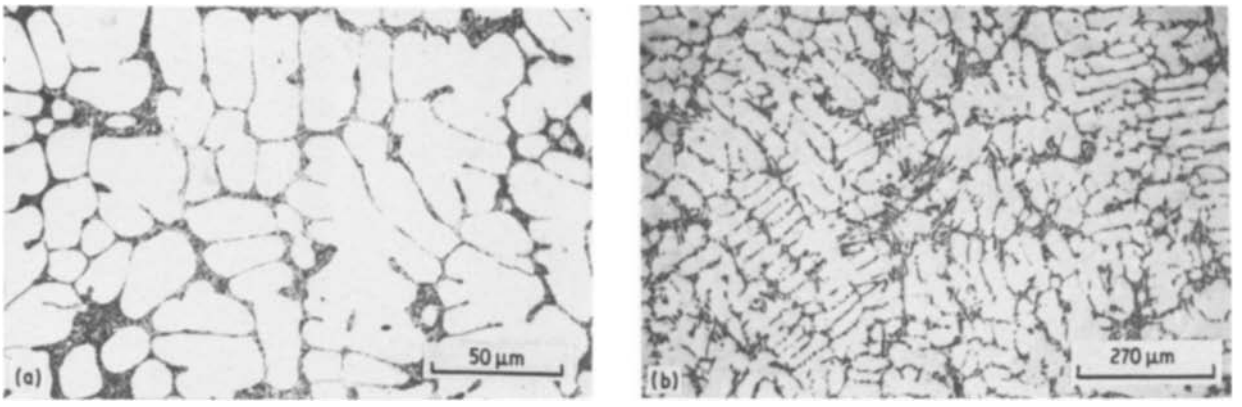

Figure 5 Microstructure of alloy A-356 (a) cast in the graphite mould and air-cooled, (b) cast in the preheated graphite mould.

The mechanical properties of alloy A-356 cast in the graphite mould are given in Table II for different conditions.

Two interesting features can be seen in Table II: (i) the moderate improvement of the properties of the "partially modified" alloy (No. 3) was greater than those of the preheated one (No. 2), and (ii) the air cooled ingots (No. 1) exhibited better mechanical properties than those of the "partially modified" alloy. The first point refers to the moderate refinement of the eutectic structure due to the addition of strontium (Al–5Sr master alloy; cf. Figs 5b and 6). The second part not only refers to the higher degree of eutectic refinement in the air cooled case, but also the the morphology of the eutectic silicon, being more or less "fine-acicular" morphology for the partially modified alloy (cf. Fig. 6). It should be mentioned that the ductility of air cooled alloys (6.2% elongation) was higher than that for alloys cast in the copper mould (2.1% elongation). This lower ductility, in the second case, refers mainly to the large "shrinkage porosity" observed in the second case due to the higher cooling rate of 5 K sec^{-1} (cf. Fig. 4b).

Fig. 7a–c shows the features of fractography as observed by optical microscopy for a longitudinal section near the fracture surface and by scanning electron microscopy as in Fig. 7b, c for alloy A-356 cast in the preheated graphite mould. Fig. 7a shows an intergranular type of brittle fracture [11, 12], it also illustrates the acicular morphology of eutectic–silicon. The general features of the fracture surface are shown in Fig. 7b in which dendritic lobes are observed in a shrinkage cavity in the upper right portion of the photomicrograph. Fig. 7c shows a cellular region that was found to be characteristic of the fracture surface. Although some features faintly suggest dimples (upper half of the photo), the higher magnification observation revealed no dimples. The formation of the cellular structure shown here is attributed to the microstructure that resulted from the freezing patterns (cf. Fig. 5b). The fracture can, in general, be rated as brittle.

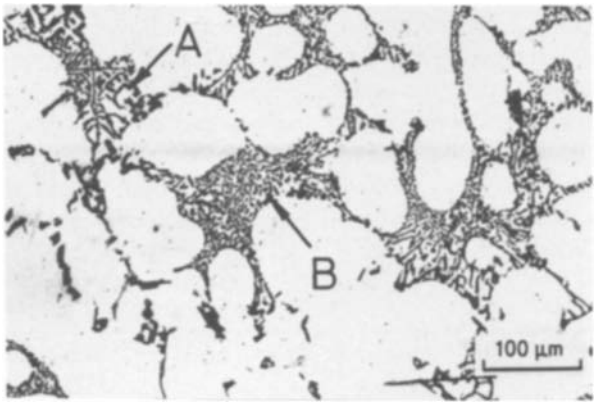

Figure 6 Microstructure of alloy A-356 cast in the preheated graphite mould plus 0.02% strontium. Notice the fineness of the eutectic structure at "A" and "B" indicating a "partial modification".

Fig. 8 shows the microstructure and the fractography of the alloy A-356 cast in sand mould. The photomicrographs in Fig. 8a, b show the microstructure of the sand cast alloys and the "modified alloys", respectively. Fig. 8a exhibits the primary α-dendrites embedded in a two-phase eutectic matrix (cf. Fig. 1). The eutectic–silicon has the acicular or needle-like morphology due to the relatively low cooling rate during solidification in sand mould (0.2 K sec^{-1}). (This acicular structure, in two dimensions, was shown to have a plate-like morphology in three dimensions.) Fig. 8b shows the modified structure after the addition of strontium (Al–5Sr master alloy) to the alloy cast in sand. It can be observed that the eutectic is very fine. Fig. 8c, d illustrate the optical fractographs on longitudinal sections near the fracture surface of the non-modified and modified alloys, respectively. While the former showed a brittle intergranular fracture, the latter showed a tendency towards transgranular fracture across the ductile α-phase. Fig. 8e, f delineate the features of the fracture surface as observed by the SEM for the sand cast and modified alloys, respectively. While Fig. 8e shows a cellular structure related to the microstructure of Fig. 8a indicating a brittle fracture, Fig. 8f shows evidence for a dimple-like pattern indicating a tendency towards ductile rupture. Bright areas marked "B" in Fig. 8f reveal a smooth ripple pattern which is believed to be an α-phase region. This smooth ripple pattern reflects the occurrence of plastic deformation in the α-phase prior to fracture. A previous research on fractography of aluminium–silicon alloy revealed two patterns [13]: (i) uneven and irregular appearance on the eutectic zones, and (ii) light network produced by slip occurring in the α-phase. The previous work also showed [13] that this plastically deformed component causes

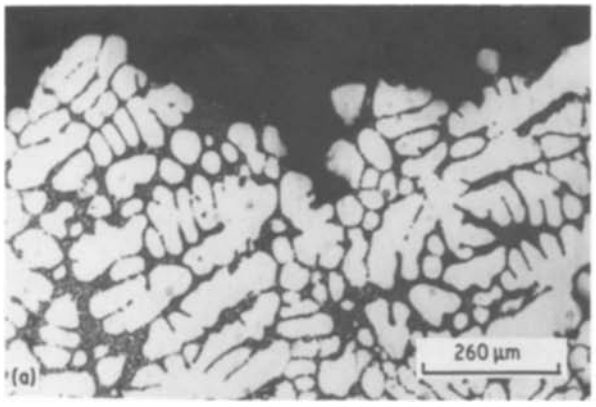

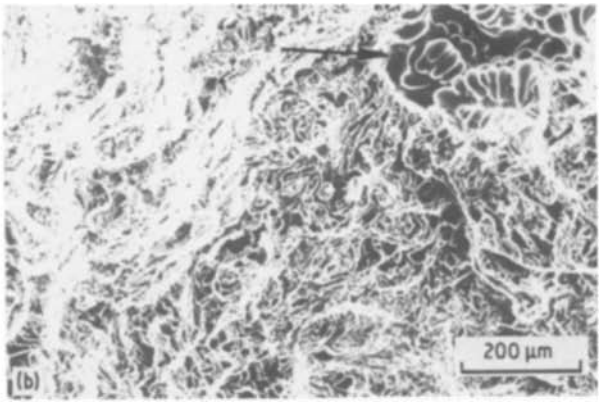

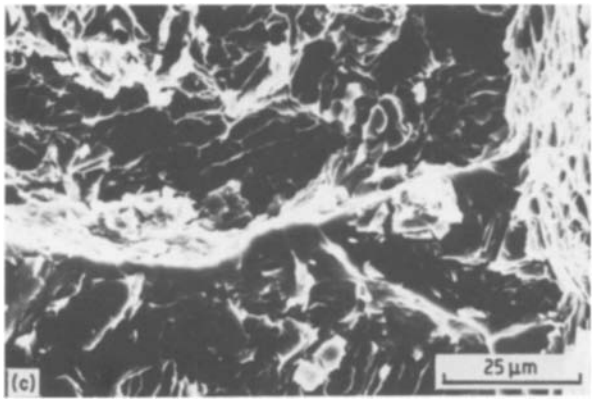

Figure 7 Fractography of alloy A-356 cast in the preheated graphite mould.

dimples to form on the bottom of which the cracked silicon was seen. However, in the previous work Al–Si–12Cu–Mg–Ni cast alloy was used which differs from the present A-356 alloy. Japanese researchers studied the effect of morphology of silicon on the fracture toughness of Al–Si alloys [14, 15], however their studies were carried out on unidirectionally produced alloys which fractured under impact tests.

The improvement of the mechanical properties, especially elongation, was clearly observed in the present investigation due to modification. It was found in the present investigation that no strontium loss was observed after melting and pouring. The mechanical properties of the sand cast and modified A-356 alloy are given in Table III. From this table it can be seen that although the yield strength was the same for both modified and non-modified alloys, the ultimate and fracture strengths increased by a value of about 35%. The ductility was remarkably increased, i.e. the ductility of the modified alloy was eight times greater than that of the non-modified one.

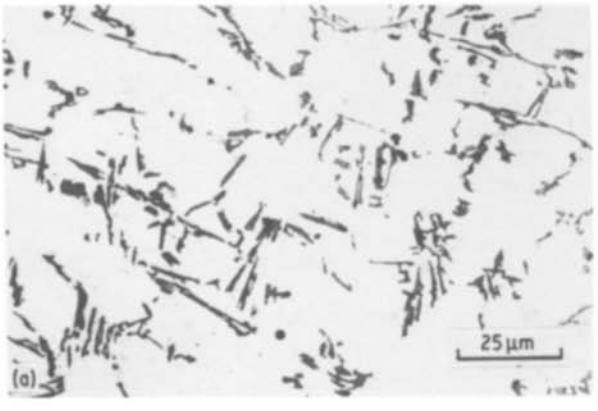

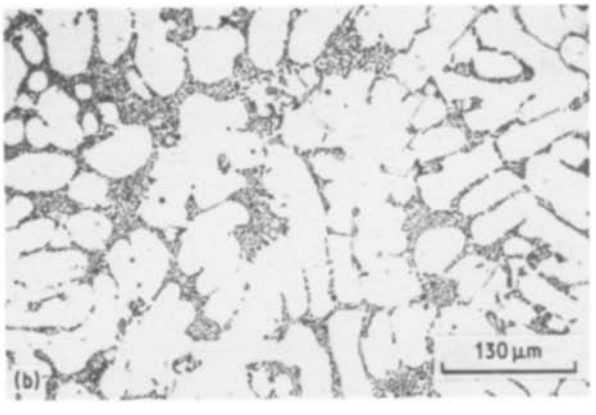

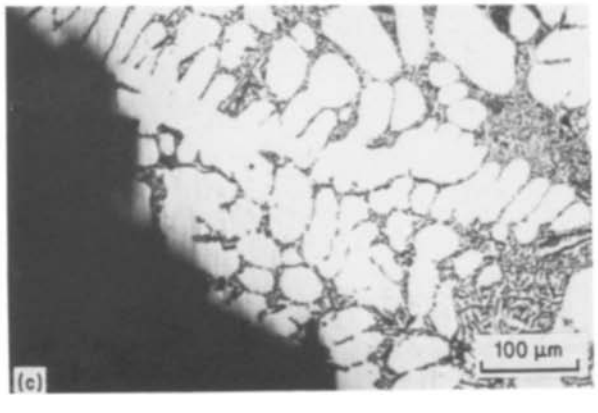

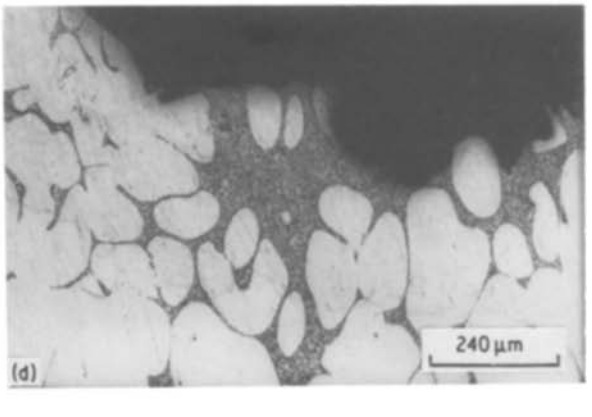

Figure 8 (a) Microstructure of alloy A-356 cast in the sand-mould, (b) modified alloy, (c) optical fractography on longitudinal sections of alloy cast in the sand mould, (d) same as in (c) for modified alloy, (e) cellular structure of fracture surface of alloy A-356 cast in the sand-mould, and (f) dimples and smooth ripple patterns observed on the modified alloy.

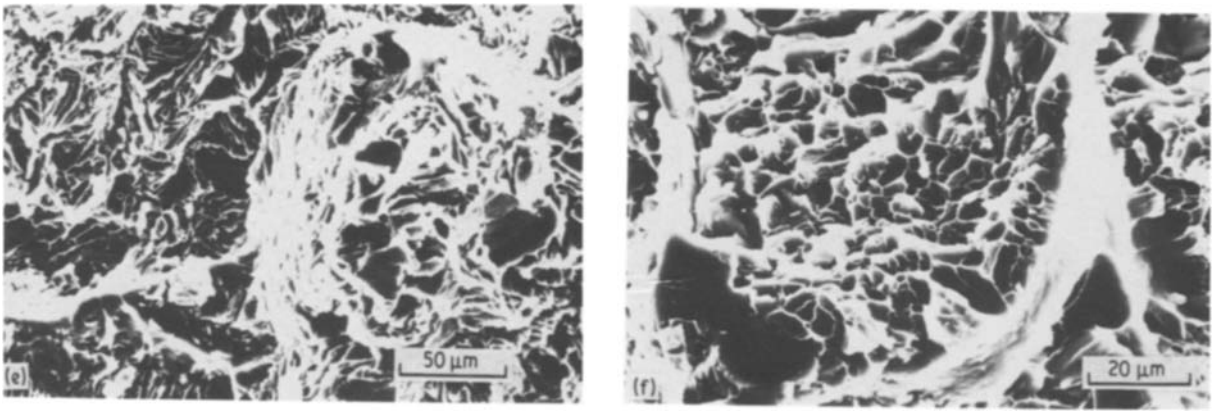

Figure 8 Continued.

The mechanical properties of the modified alloy, in the present research, were superior to those modified with sodium [4], and additionally, the ductility of the present modified alloy was superior to that modified with strontium element [7].

4. Conclusions

For aluminium–silicon alloy A-356 used in the present research, the following conclusions can be drawn.

1. Decreasing the cooling rate during solidification increases the "degree of modification" reaching an optimum modification at a cooling rate of 0.2 K sec^{-1}, using Al–5 mass % Sr master alloy in the present study.
2. Mechanical properties of the modified alloys are significantly higher than those of the non-modified ones, especially ductility in the former which increased to eight times the value of the latter.
3. Mechanical properties of the modified alloys including the yield and ultimate strengths and the ductility are higher than those reported previously for alloy A-356 modified with sodium. Moreover, the ductility of the present modified alloy is a little bit higher than that for alloy A-356 modified with strontium element.

TABLE III Mechanical properties of the sand cast and modified A-356 alloy

Alloy A-356	σ_y (MPa)	UTS (MPa)	σ_f (MPa)	Elongation (%)
Sand cast	110	15	150	1.8
Modified	110	210	200	15

4. The fractography of the present alloy revealed tendency to ductile rupture. Evidence for the transgranular type of fracture was exhibited. Additionally, a dimple-pattern could clearly be seen on the fracture surface, by SEM, of the modified alloy.

References

1. A. PACZ, USA Patent No. 1387900 (1920).
2. M. HANSEN, "Constitution of Binary Alloys" 2nd Edn (McGraw-Hill, New York, Toronto, London, 1958) 132.
3. G. A. CHADWICK, *Prog. Mater. Sci.* **12** (1965) 99.
4. A. HELLAWELL, *ibid.* **15** (1970) 3.
5. ASM Metals Handbook, "Metallography, Structures and Phase-Diagrams", Vol. 8 (Ohio, 1973) p. 263.
6. L. F. MONDOLFO, "Aluminium Alloys", 1st Edn (Butterworths, London, Boston, Sydney, Toronto, 1976).
7. J. CHARBONNIER *et al.*, *AFS Int. Cast Metals J.* **3** (1978) 17.
8. B. CLOSSET and J. E. GRUZLESKI, *AFS Trans.* **89** (1981) 801.
9. *Idem, Metall. Trans. A* **13A** (1982) 945.
10. P. D. HESS and E. V. BLACKMUN, *AFS Trans.* **83** (1975) 87.
11. G. F. PITTINATO *et al.* "SEM/TEM Fractography Handbook" (McDonnell Douglass Astronautics Co., Huntigon Beach, California, 1975).
12. ASM Metals Handbook, "Fractography and Atlas of Fracture", 8th Edn (Ohio, 1974).
13. P. REZNICEK and K. STETINA, *Praktische Metallographie* **16** (1979) 59.
14. E. KATO and T. KOBAYASHI, *Trans. JIM* **30** (1980) 147.
15. *Idem, ibid.* **30** (1980) 140 (in Japanese).

Received 26 March
and accepted 21 July 1986